Journal of Medicinal Chemistry

Subscriber access provided by American Chemical Society

Article

Inhibition of Carboxylesterases by Benzil (Diphenylethane-1,2-dione) and Heterocyclic Analogues Is Dependent upon the Aromaticity of the Ring and the Flexibility of the Dione Moiety

Janice L. Hyatt, Vanessa Stacy, Randy M. Wadkins, Kyoung Jin P. Yoon, Monika Wierdl, Carol C. Edwards, Matthias Zeller, Allen D. Hunter, Mary K. Danks, Guy Crundwell, and Philip M. Potter

J. Med. Chem., **2005**, 48 (17), 5543-5550• DOI: 10.1021/jm0504196 • Publication Date (Web): 08 July 2005

Downloaded from http://pubs.acs.org on March 28, 2009

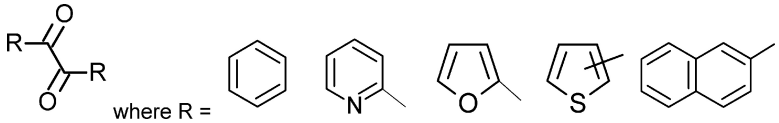

More About This Article

Additional resources and features associated with this article are available within the HTML version:

- Supporting Information
- Links to the 4 articles that cite this article, as of the time of this article download
- Access to high resolution figures
- Links to articles and content related to this article
- Copyright permission to reproduce figures and/or text from this article

View the Full Text HTML

ACS Publications
High quality. High impact.

Journal of Medicinal Chemistry is published by the American Chemical Society. 1155 Sixteenth Street N.W., Washington, DC 20036

Inhibition of Carboxylesterases by Benzil (Diphenylethane-1,2-dione) and Heterocyclic Analogues Is Dependent upon the Aromaticity of the Ring and the Flexibility of the Dione Moiety

Janice L. Hyatt,[†] Vanessa Stacy,[‡] Randy M. Wadkins,[§] Kyoung Jin P. Yoon,[†] Monika Wierdl,[†] Carol C. Edwards,[†] Matthias Zeller,[||] Allen D. Hunter,[||] Mary K. Danks,[†] Guy Crundwell,[‡] and Philip M. Potter[†,*]

Department of Molecular Pharmacology, St. Jude Children's Research Hospital, 332 N. Lauderdale, Memphis, Tennessee 38105, Department of Chemistry, Central Connecticut State University, New Britain, Connecticut 06050, Department of Chemistry and Biochemistry, University of Mississippi, University, Mississippi 38677, and Department of Chemistry, Youngstown State University, Youngstown, Ohio 44555

Received May 3, 2005

Benzil has been identified as a potent selective inhibitor of carboxylesterases (CEs). Essential components of the molecule required for inhibitory activity include the dione moiety and the benzene rings, and substitution within the rings affords increased selectivity toward CEs from different species. Replacement of the benzene rings with heterocyclic substituents increased the K_i values for the compounds toward three mammalian CEs when using *o*-nitrophenyl acetate as a substrate. Logarithmic plots of the K_i values versus the empirical resonance energy, the heat of union of formation energy, or the aromatic stabilization energy determined from molecular orbital calculations for the ring structures yielded linear relationships that allowed prediction of the efficacy of the diones toward CE inhibition. Using these data, we predicted that 2,2′-naphthil would be an excellent inhibitor of mammalian CEs. This was demonstrated to be correct with a K_i value of 1 nM being observed for a rabbit liver CE. In addition, molecular simulations of the movement of the ring structures around the dione dihedral indicated that the ability of the compounds to inhibit CEs was due, in part, to rotational constraints enforced by the dione moiety. Overall, these studies identify subdomains within the aromatic ethane-1,2-diones, that are responsible for CE inhibition.

Introduction

Carboxylesterases (CEs) are ubiquitously expressed enzymes thought to be responsible for the detoxification of xenobiotics.[1] In man, they metabolize a wide variety of compounds, including the clinically useful drugs CPT-11, capecitabine, meperidine, etc., as well as the illicit street drugs heroin and cocaine.[2−10] In general, CEs are expressed in tissues likely to be exposed to such agents including the liver, small intestine, liver, kidney, etc., although in humans very little CE is expressed in the blood.[11,12] This is in contrast to small mammals where very high levels of CE can be detected in the plasma of mice, rats, and rabbits.[12−14]

We have recently attempted to identify selective inhibitors of CEs, with the goal of developing compounds for clinical use that would alter the distribution and clearance of esterified drugs. Potentially, such agents could be used to ameliorate the toxicity observed with heroin overdose or block the delayed diarrhea that accompanies CPT-11 administration.[15−17] In a small scale screen of a library developed by Telik Inc. using their Target Related Affinity Profiling (TRAP),[18−20] we identified an analogue of benzil (diphenylethane-1,2-dione; **2**) as a potent inhibitor of mammalian CEs.[21] The parent compound benzil inhibited the catalysis of *o*-nitrophenyl acetate (*o*-NPA), 4-methylumbelliferone acetate, and CPT-11 by two human and one rabbit liver CE. Subsequent biochemical analyses indicated that the ethane-1,2-dione moiety was essential for enzyme inhibition, and that the potency of the compound was dependent upon the presence of the benzene rings.[21] In addition, numerous analogues of benzil were identified that demonstrated selective inhibition of the mammalian CEs. QSAR analysis indicated that the selectivity afforded by these compounds was due, in part, to steric interactions and clashes within the active sites of the proteins. Benzil, and all of the analogues containing substitutions within the benzene rings, demonstrated no inhibitory activity toward human acetylcholinesterase (hAcChE) or butyrylcholinesterase (hBuChE).[21]

During the course of these studies, we synthesized and assessed the ability of dione analogues containing heteroaromatic rings to inhibit CEs. Here we present evidence that indicates that the ability of these diones to inhibit mammalian CEs is due, in part, to the aromaticity of the ring structure and the rotation of these moieties about the dione chemotype. Use of this information for the prediction and identification of more potent CE inhibitors has been achieved, resulting in the synthesis and evaluation of 2,2′-naphthil (**11**) as a potent selective inhibitor of these enzymes. In addition, analysis of CE inhibition by 2,2′-thenil (**4**) and bromo-

* Corresponding author: Dr. Philip M. Potter, Department of Molecular Pharmacology, St. Jude Children's Research Hospital, 332 N. Lauderdale, Memphis, TN 38105; Tel: 901-495-3440; Fax: 901-521-1668; E-mail: phil.potter@stjude.org.
[†] St. Jude Children's Research Hospital.
[‡] Central Connecticut State University.
[§] University of Mississippi.
[||] Youngstown State University.

10.1021/jm0504196 CCC: $30.25 © 2005 American Chemical Society
Published on Web 07/08/2005

substituted analogues (**6**, **7**) indicated the addition of the halogen atoms increased the potency of the compounds probably by increasing the hydrophobicity of the molecules.

Experimental Section

Chemicals. Benzil (**2**), benzoin (**1**), furil (**8**), furoin (**9**), and 2,2′-pyridil (**10**) were all obtained from Sigma Aldrich (St. Louis, MO). 2,2′-Thenoin (**3**) and 2,2′-thenil (**4**) were purchased from Alfa Aesar (Ward Hill, MA), and 2,2′-naphthil (**11**) was obtained from Industrial Research Ltd. (Auckland, New Zealand). 3-Thiophenecarboxaldehyde and the 4-bromo- and 5-bromo-substituted analogues were all purchased from Sigma Aldrich.

Synthesis of 3,3′-Thenil Analogues. 3,3-Thenil (**5**), 4,4′-dibromo-2,2′-thenil (**6**), and 5,5′-dibromo-2,2′-thenil (**7**) were synthesized by condensation of the substituted 3-thiophenecarboxaldehyde (0.1 mol) in the presence of thiamine hydrochloride (0.009 mol) and alcoholic sodium hydroxide to yield the thenoin,[22] with subsequent oxidation using copper acetate (0.001 mol) and ammonium nitrate (0.09 mol) in 80% acetic acid.[23] Products were purified by recrystallization, melting points were determined using a Mel-temp (Barnstead International, Dubuque, IA), and purity and structures were assessed by TLC, NMR, and total C, H, N analysis.

3,3′-Thenil (1,2-dithien-2-ylethane-1,2-dione; 5). 3,3′-Thenil was synthesized from 1,2-dithien-3-ylethane-1-hydroxy-2-one to yield a pale yellow solid (yield 68%). Physical and NMR parameters of **5**: mp 80°C; ^{1}H NMR (400 MHz, $CDCl_3$) δ 8.33 (d, 2H), 7.67 (d, 2H), 7.37 (m, 2H).

4,4′-Dibromo-2,2′-thenil (1,2-bis(4-bromothien-2-yl)-ethane-1,2-dione; 6). 4,4′-Dibromo-2,2′-thenil was synthesized from 1,2-bis(4-bromothien-2-yl)ethane-1-hydroxy-2-one to yield a yellow solid (yield 33%). Physical and NMR parameters of **6**: mp 164−165°C; ^{1}H NMR (400 MHz, $CDCl_3$) δ 8.04 (m, 2H), 7.73 (m, 2H).

5,5′-Dibromo-2,2′-thenil (1,2-bis(5-bromothien-2-yl)-ethane-1,2-dione; 7). 5,5′-Dibromo-2,2′-thenil was synthesized from 1,2-bis(5-bromothien-2-yl)ethane-1-hydroxy-2-one to yield a yellow solid (yield 26%). Physical and NMR parameters of **7**: mp 136−137°C; ^{1}H NMR (400 MHz, $CDCl_3$) δ 7.91 (m, 2H), 7.18 (m, 2H).

Enzymes. Pure human liver CE (hCE1) and rabbit liver CE (rCE) were prepared as previously described.[24] Partially pure (>50%) human intestinal CE (hiCE) was produced from media harvested from *Spodoptera frugiperda* sf21 cells infected with baculovirus encoding a secreted form of the protein. Since this medium is protein free, the only CE present within this sample is hiCE. hAcChE and hBuChE were purchased from Sigma Biochemicals (St. Louis, MO).

Inhibition of Carboxylesterases. CE inhibition was assessed using a spectrophotometric assay with 3mM *o*-NPA as a substrate.[21,25] Typically, enzymes were incubated with substrate and inhibitor in 50 mM HEPES pH7.4, and the data was automatically transferred to computer spreadsheet for analysis. Routinely, at least eight inhibitor concentrations were used ranging from 1 pM to 100 μM, and each data point was performed in duplicate. Data were analyzed using the following equation:[26]

$$i = \frac{[\mathrm{I}][\mathrm{S}](1-\beta) + K_\mathrm{s}(\alpha-\beta)}{[\mathrm{I}]([\mathrm{S}] + \alpha K_\mathrm{s}) + K_\mathrm{i}(\alpha[\mathrm{S}] + \alpha K_\mathrm{s})}$$

where i = fractional inhibition; [S] = substrate concentration; [I] = inhibitor concentration; α = change in affinity of substrate for enzyme, β = change in the rate of enzyme substrate complex decomposition, K_s is the dissociation constant for the enzyme−substrate complex, and K_i is the dissociation constant for the enzyme−inhibitor complex. Subsequently, results were plotted using GraphPad Prism software, and K_i values were calculated using the appropriate enzyme inhibition model.[21,25]

Inhibition of Acetylcholinesterase and Butyrylcholinesterase. The ability of compounds to inhibit hAcChE and hBuChE was performed as previously described using either 1 mM acetylthiocholine (AcTCh) or 1 mM butyrylthiocholine (BuTCh) as substrates, respectively.[27−30]

Calculation of Aromatic Stabilization Energies. Empirical resonance energies for the compounds described in this article were obtained from Gordon and Ford.[31] Heat of union energies were obtained or calculated using the method described by Dewar and Holder.[32] Molecular orbital calculations were performed using the PM3 Hamiltonian of MOPAC.[33−35]

Molecular Simulations of the Diones. Molecular simulations were run for the dione analogues using the MM3 module of Alchemy (Tripos Inc., St. Louis, MO). Briefly, molecules were minimized using PM3 geometry minimization and then subjected to the molecular dynamics run. The dihedral angle for the dione bonds [(O)CC(O)] was measured over 15 ps using a time step of 1 fs at an initial temperature of 293 K. Data were recorded every 10 fs.

X-ray Crystallography. The crystal structures of 4,4′-dibromo-2,2′-thenil (**6**) and 5,5′-dibromo-2,2′-thenil (**7**) were determined from single-crystal X-ray diffraction omega scan data collected at 100 K on a Bruker AXS SMART Apex 512k CCD diffractometer equipped with fine-focus sealed tube Mo K X-ray source (λ = 0.71073 Å). Both sets of data were corrected for absorption effects using SADABS.[36] The R_int for the 4,4′-dibromo- and 5,5′-dibromo-2,2′-thenils were 0.0750 and 0.0499, respectively. Data workup, structure solution, refinement, and the generation of cif files were performed using SHELXTL.[37] In both molecules, all non-hydrogen atoms were identified from initial direct methods solutions and were refined anisotropically. Hydrogen atoms were placed at a C−H distance of 0.95 Å, and bond lengths and angles fell within normal, expected values. (The full details of crystal structure determinations such as data collection parameters, all bond lengths, bond and torsion angles, and refinement statistics are available as Supporting Information.)

Results

K_i Values for Aromatic 1,2-Hydroxyketones and Corresponding Diones. We have previously reported the K_i values for benzil (**2**) and benzoin (**1**) for CEs with a variety of esterase substrates and different mammalian CEs and demonstrated that the former was a potent inhibitor of these proteins.[21] Table 1 depicts the structures of the aromatic ethane-1-hydroxy-2-ones and their corresponding diones that have been assessed in this study. As indicated in Table 2, the 1,2-hydroxyketones were generally poor inhibitors of *o*-NPA metabolism by CEs, whereas the diones analogues were much more potent selective inhibitors of these enzymes. We did not assess the ability of 2,2′-pyridoin to inhibit CEs, due to its propensity to oxidize to 2,2′-pyridil.

Correlation between K_i Values and Aromaticity of Ring Substituents. A trend was observed that indicated that the potency of inhibition of CEs by the diones was related to the level of stabilization of the electrons in the aromatic rings. Therefore, we plotted the log K_i values versus the aromatic stabilization energy afforded by the ring systems present within the different analogues. Three different sets of data were chosen for the resonance energies. The first was based upon empirical resonance energies for the compounds (15.8, 28.7, 23, and 36 kcal/mol for furan, thiophene, pyridine, and benzene, respectively[31]). The second was based upon heats of union of atomic pairs using nonaromatic precursors (12.1, 16.5, 25.6, and 28.3kcal/mol for furan, thiophene, pyridine, and benzene, respectively[32]). The third was based upon molecular orbital

Table 1. Structures of Compounds Assessed for CE Inhibition

ID	Name	Structure
1	Benzoin (1,2-diphenylethane-1-hydroxy-2-one)	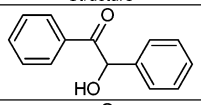
2	Benzil (1,2-diphenylethane-1,2-dione)	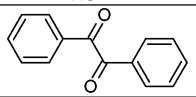
3	2,2'-Thenoin (1,2-dithien-2-ylethane-1-hydroxy-2-one)	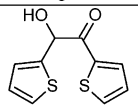
4	2,2'-Thenil (1,2-dithien-2-ylethane-1,2-dione)	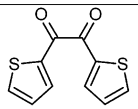
5	3,3'-Thenil (1,2-dithien-3-ylethane-1,2-dione)	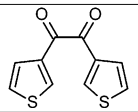
6	4,4'-dibromo-2,2'-thenil (1,2-bis(4-bromothien-2-yl)ethane-1,2-dione)	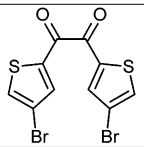
7	5,5'-dibromo-2,2'-thenil (1,2-bis(5-bromothien-2-yl)ethane-1,2-dione)	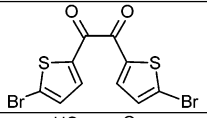
8	Furoin (1,2-(di-2-furyl)-ethane-1-hydroxy-2-one)	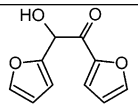
9	2,2,-Furil (1,2-di-2-furylethane-1,2-dione)	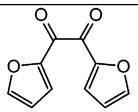
10	2,2'-Pyridil (1,2-dipyridin-2-ylethane-1,2-dione)	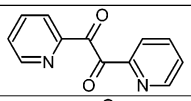
11	2,2'-Naphthil (1,2-di-2-naphthylethane-1,2-dione)	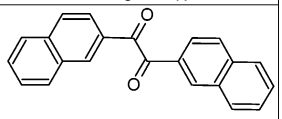

calculations with MOPAC using the PM3 Hamiltonian. This gave resonance energies of 8.7, 7.9, 16.2, and 23.0 kcal/mol for furan, thiophene, pyridine, and benzene, respectively

As indicated in Figure 1, good correlations were observed between the K_i values and the thermodynamic parameters, with r^2 values of 0.841, 0.897, and 0.888 being obtained for hiCE, hCE1, and rCE, respectively, when using the empirical resonance energies (Figure 1A). With data derived from aromatic energies calculated from the heats of union, r^2 values of 0.972, 0.936, and 0.951 were obtained with the same enzymes, respectively (Figure 1B). Finally, using the data calculations from MOPAC, correlation coefficients of 0.936, 0.834, and 0.877 were generated using K_i values from hiCE, hCE1, and rCE, respectively (Figure 1C).

Since the r^2 values were greater than 0.80, we reasoned that these correlations might have some predictive value in calculating the K_i values of other aromatic ethane-1,2-diones. Using linear regression analysis, we predicted that 2,2′-naphthil (**11**) would be a potent inhibitor of all three CEs. We therefore calculated the predicted K_i values for CE inhibition with 2,2′-naphthil (**11**) using energy values of 61, 47.7, and 41.6 kcal/mol for naphthalene from empirical resonance, heat of union, or molecular orbital calculations, respectively. Table 3 indicates the predicted and observed values of the K_i values for 2,2′-naphthil (**11**) using the three mammalian CEs. As can be seen, the K_i values derived from the equations obtained from the above curve fits did not accurately predict the observed values for hiCE or hCE1. We believe that this is due to that fact that both of these proteins have relatively narrow entrances to their active sites [10] that would impede the passage of large molecules, such as 2,2′-naphthil (**11**), to the catalytic residues. In contrast, the predicted K_i values for rCE with this compound using the equations derived from the empirical resonance energy plot (1.03 nM), the heat of union calculations (1.64 nM), or the MOPAC analysis (1.56 nM) were very close to the observed value (1.04 ± 0.09 nM). It would appear that the predictive power of this approach may be sufficient to identify novel rCE inhibitors based upon the 1,2-dione structure.

Correlation between K_i Values and Flexibility of Dione Bond. Analysis of the rotation of the dione bond using molecular dynamic simulations suggested that the potency of the inhibitors might be related to the flexibility and/or the dihedral angle adopted in the minimized structure. We therefore examined the angle for the dione bond for 15 ps using the MM3 molecular mechanics force field, with a time step of 1 fs, a temperature of 293 K, and data were recorded every 10 fs. As indicated in Figure 2, with 2,2′-furil (**9**), 2,2′-thenil (**4**), and 2,2′-pyridil (**10**), we observed pronounced oscillations between two low-energy conformations during the dynamics simulation. As these analogues are generally poorer CE inhibitors, it may be that loss of flexibility of the dione moiety upon binding to CEs results in a significantly unfavorable conformational entropy loss. For the more rigid analogues such as benzil (**2**) and 2,2′-naphthil (**11**), the oscillation around the O−C−C−O dihedral was much less pronounced. In general, as the compounds became poorer inhibitors of the CEs, the time taken for rotation about the dihedral bond to minimize, increased (Figure 2).

Also, there were considerable differences in the final angle adopted by the dione moiety following the dynamics minimization. A general trend was that inhibitors with a low K_i value for the mammalian CEs obtained a final dihedral angle of ∼230° (or −130°). Significant deviation from this value resulted in inhibitors with markedly less ability to inhibit, and Figure 3 shows the approximate dependence of K_i on the angle adopted. However, we do not have enough analogues to establish the actual angle energy function. Overall, however, molecular simulations of unknown compounds, examining both the dione flexibility and the dihedral angle, might be useful in a predictive fashion to allow identification of novel CE inhibitors.

Inhibition of CEs by Thenil and Its Brominated Derivatives. Analysis of the inhibition of the mammalian CEs by 2,2′- (**3**) and 3,3′-thenil (**5**) indicated that

Table 2. K_i Values for Inhibition of by hiCE, hCE1, rCE, hAcChE, and hBuChE by Aromatic Ethane-1-hydroxy-2-ones and Their Corresponding Diones[a]

compound	hiCE K_i (nM)	hCE1 K_i (nM)	rCE K_i (nM)	hAcChE K_i (nM)	hBuChE K_i (nM)
benzoin (**1**)	2220 ± 460	7250 ± 2370	>100000	>100000	>100000
benzil (**2**)	14.7 ± 1.9	45.1 ± 3.2	103 ± 19	>100000	>100000
2,2′-thenoin (**3**)	5610 ± 1260	1660 ± 140	4540 ± 1040	>100000	>100000
2,2′-thenil (**4**)	1040 ± 190	212 ± 29	874 ± 53	>100000	>100000
3,3′-thenil (**5**)	6540 ± 580	365 ± 18	2410 ± 100	>100000	>100000
4,4′-dibromo-2,2′-thenil (**6**)	57.3 ± 8.1	30.0 ± 2.0	2.2 ± 0.5	>100000	>100000
5,5′-dibromo-2,2′-thenil (**7**)	237 ± 48	210 ± 50	7.0 ± 2.1	>100000	>100000
2,2′-furoin (**8**)	>100000	>100000	>100000	>100000	>100000
2,2′-furil (**9**)	8000 ± 790	1170 ± 450	8480 ± 1170	>100000	>100000
2,2′-pyridil (**10**)	152 ± 11	126 ± 12	484 ± 34	>100000	>100000

[a] *o*-NPA was used as a substrate for the CEs, and AcTCh and BuTCh were used for hAcChE and hBuChE, respectively.

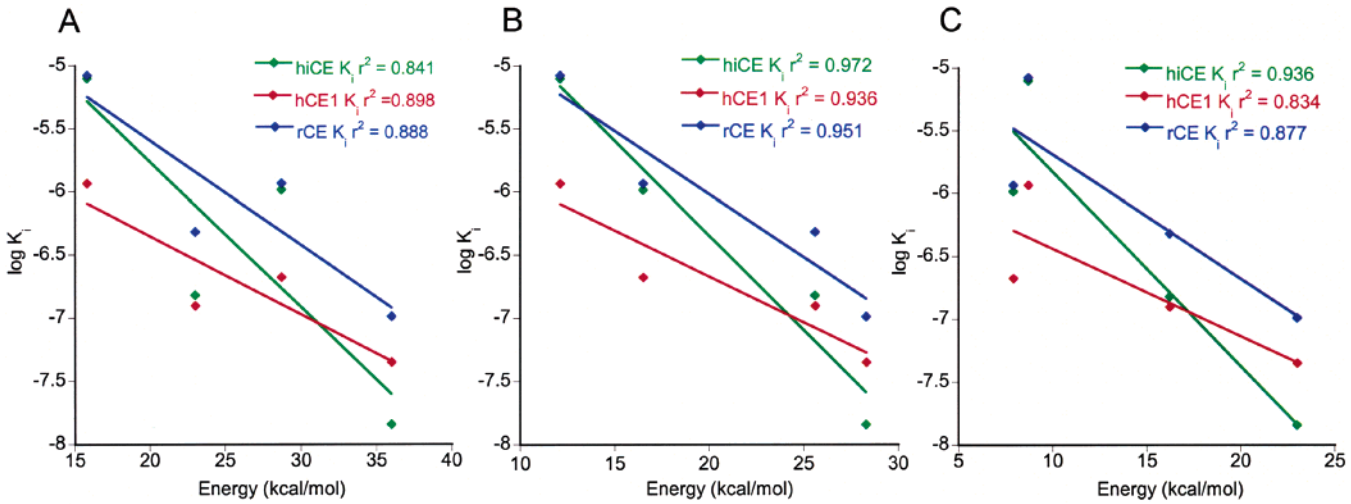

Figure 1. Plot of empirical resonance energy (A), heat of union of atomic pairs (B), and molecular orbital energies (C) for the aromatic rings, versus the observed K_i values for the diones. Linear regressions for the data derived from hiCE (green line), hCE1 (red line), and rCE (blue line) are shown.

Table 3. Observed and Predicted K_i Values (nM) for Inhibition of *o*-NPA Metabolism by CEs with 2,2′-Naphthil (**11**)[a,b]

hiCE				hCE1				rCE			
	predicted K_i value (nM)				predicted K_i value (nM)				predicted K_i value (nM)		
observed	empirical[c]	HOU[d]	MO[e]	observed	empirical	HOU	MO	observed	empirical	HOU	MO
85.0 ± 15.3	0.034	0.032	0.020	255 ± 33	1.29	2.06	2.32	1.04 ± 0.09	1.03	1.64	1.56

[a] Predicted K_i values were calculated from the equations obtained from plots of log K_i versus energy values (see Figure 1). [b] Energy values of 61.0, 47.7, or 41.6kcal/mol were used to calculate the predicted K_i values for the empirical, heat of union, or molecular orbital datasets, respectively. [c] Empirical resonance energy calculation.[31] [d] Heat of union calculation.[32] [e] Molecular orbital calculation.

the former compound was ~6- to 1.7-fold more potent as an inhibitor when using *o*-NPA as a substrate (Table 2). In addition, substitution in the thiophene rings with bromine, decreased the K_i values up to 400-fold. While substitution with the halogen significantly reduced the K_i for rCE, less pronounced effects were observed with hiCE and hCE1. For example, 5,5′-dibromo-2,2′-thenil (**7**) was ~4-fold more potent at inhibiting hiCE as compared to 2,2′-thenil (**4**), and both compounds demonstrated very similar K_i values for hCE1. In contrast, the former compound was ~125-fold more efficient at inhibiting *o*-NPA metabolism by rCE, as compared to 2,2′-thenil. Additionally, 4,4′-dibromo-2,2′-thenil (**6**) was considerably more potent at inhibition of all three CEs, with this compound yielding the lowest K_i (2.2 ± 0.5 nM) for rCE, for all of the compounds tested.

Analysis of the rotation of the molecules around the dione dihedral was performed as described above and for the unsubstituted thenils, increased rotation was observed with the poorer inhibitor (3,3′-thenil; **5**) as compared to 2,2′-thenil (**4**) (Figure 4A). However, substitution of bromine atoms resulted in dramatically increased movement around these bonds (Figure 4B), and this persisted for the entire period of the molecular dynamics run (15 ps). No obvious correlation was seen between inhibitor potency and the dihedral rotation for the brominated compounds (Figure 4B). Interestingly, however, the final angle adopted by the dione in the MD simulations was close to 230° for both of the bromo derivatives and 2,2′-thenil (**4**). These compounds were much better inhibitors than 3,3′-thenil (**5**) which adopted a final angle of ~260°.

X-ray Crystallography of Bromothenil Analogues. Since we saw differences in the ability of the bromothenils to inhibit CEs, we ascertained the X-ray structures of the molecules to determine whether differences in the geometry of the compounds might account for the differences in inhibitory activity. Specific refinement details for 4,4′-dibromo-2,2′-thenil (**6**) and 5,5′-dibromo-2,2′-thenil (**7**) were as follows. By inspec-

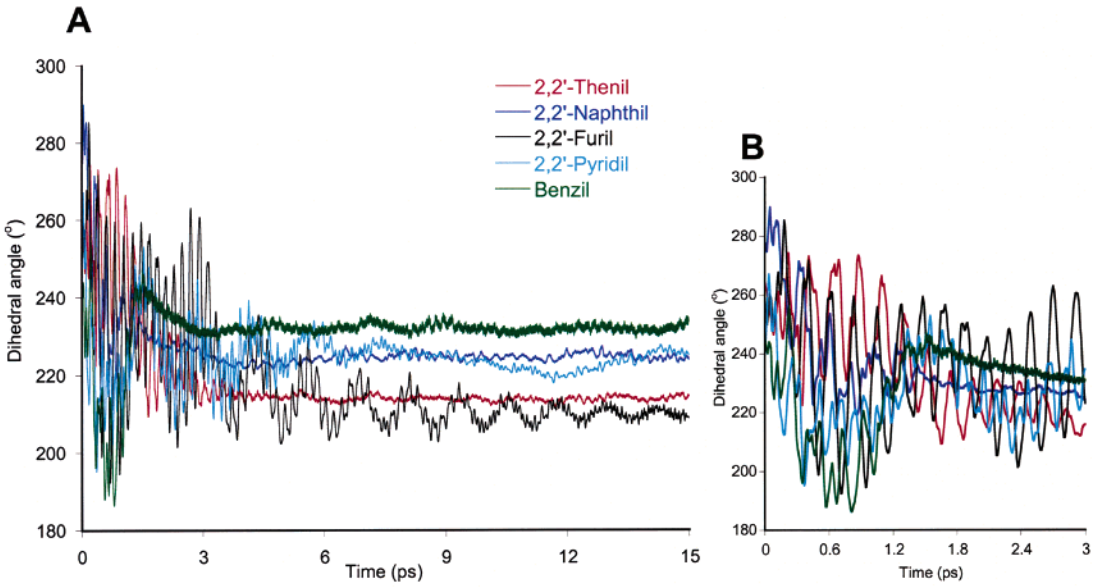

Figure 2. Plot of the dihedral angel versus time for molecular simulations of the diones. In panel A, the variation in the angle is indicated for benzil (black line; **2**), 2,2′-naphthil (green line; **11**), pyridil (dark blue line; **10**), 2,2′-thenil (red line; **4**), and furil (cyan line; **9**). The inset (panel B) indicates the movement within the first 3 ps of the molecular dynamics run.

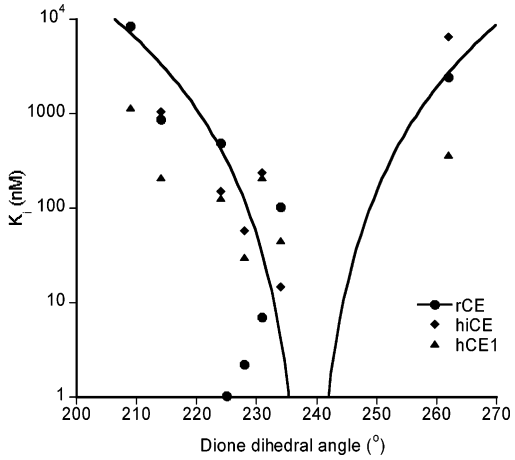

Figure 3. Plot of the final dione dihedral angle versus the K_i values for the CEs. Data were fitted to the following equation ($y = m_1(m_0 - m_2)^4$), and r^2 values of 0.92, 0.96, and 0.92 were obtained for hiCE (◆), hCE1 (▲), and rCE (●), respectively. For clarity, only the best fit line for rCE is indicated (black).

tion of systematic absences in the diffraction pattern, crystals of 4,4′-dibromo-2,2′-thenil (**6**) were assigned to the space group $P2_12_12$. To ensure the correct designation of polarity, the Flack parameter was refined.[38] Structure refinement yielded one-half of a molecule in the asymmetric unit that sits on a 2-fold axis. The atoms that make up the half molecule were essentially planar with the rms deviation of atoms from the plane being only 0.0338 Å. As seen in the ORTEP[39] model shown in Figure 5, the ring sulfur and keto oxygen adopt a cis configuration in 4,4′-dibromo-2,2′-thenil (**6**). By inspection of systematic absences in the diffraction pattern, crystals of 5,5′-dibromo-2,2′-thenil (**7**) were determined to be of space group $P2_12_12_1$. Once again, the Flack parameter was refined to ensure the correct designation of the polar axis. For 5,5′-dibromo-2,2′-thenil (**7**), one molecule resides in the asymmetric unit, and it is essentially planar, having a rms deviation for all the atoms in the plane of 0.0755 Å. However, each half of the ethane-dione is more planar. Atoms O1, Br1, S1, and C1−C5 have rms deviations from planarity of 0.0396 Å; whereas atoms O2, Br2, S2, and C6−C10 have rms deviations of 0.0307 Å. Both of these values are not only in agreement with 4,4′-dibromo-2,2′-thenil (**6**), but also with the vast majority of symmetric aromatic ethane-diones in the Cambridge Structural Database (March, 2004). ORTEP depictions of 4,4′-dibromo-2,2′-thenil (**6**) and 5,5′-dibromo-2,2′-thenil (**7**) are shown in Figure 5.

Discussion

Until recently, the discovery of selective CE inhibitors has been somewhat elusive, with many compounds inhibiting other esterases, such as hAcChE and hBuChE. These chemicals, that include simple organophosphates such as bis(4-nitrophenyl) phosphate, as well as the pesticides malathion (*o*,*o*′-dimethyl *S*-(1,2-dicarbethoxyethyl)thiothionophosphate) and pirimphos (*o*-(2-(diethylamino)-6-methyl-4-pyrimidinyl)-*o*,*o*-dimethyl phosphorothioate), and the nerve gases Sarin (isopropylmethylphosphonofluoridate), Tabun (ethyl dimethylamidocyanidophosphate), and VX (*S*-[2-(diisopropylamino)ethyl] *o*-ethyl methylphosphonothioate), are all potent inhibitors of many different mammalian esterases. In a directed screen of several hundred small molecules, we identified that diphenylethane-1,2-diones analogues were potent inhibitors of CEs, that demonstrated no activity against hAcChE or hBuChE.[21] In this paper, we have extended our studies to examine the contribution of the aromatic rings toward enzyme inhibition. In addition, we have assessed the role of thermodynamic and molecular dynamic parameters in predicting the ability of the ethane-1,2-diones to inhibit mammalian CEs.

Analysis of the K_i values for the inhibition of *o*-NPA metabolism by CEs with heteroaromatic diones suggested that these results might be correlated to the aromatic nature of the ring structure. Previous reports have suggested that for esterase substrates, the catalytic efficiency for their turnover was related to the log

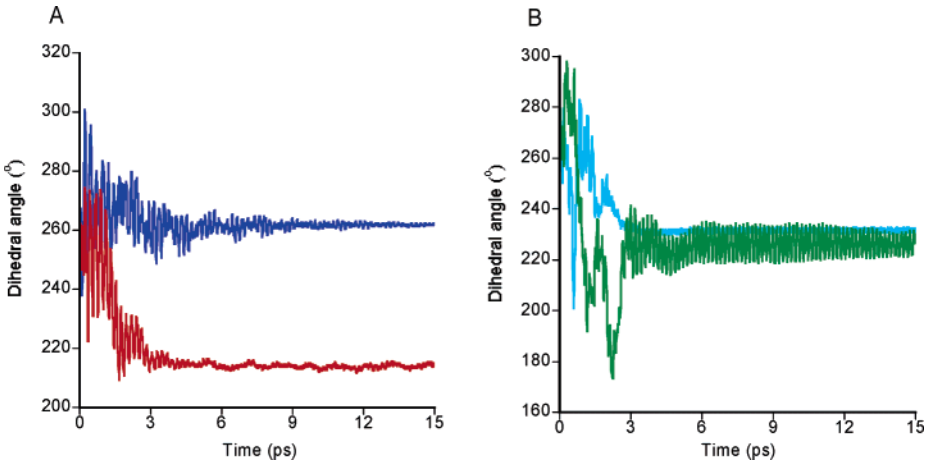

Figure 4. Plot of the dihedral angle versus time for molecular simulations of the thiophene-based ethane-1,2-diones. The variation in the angle is indicated for 2,2′-thenil (red line, panel A; **4**), 3,3′-thenil (blue line, panel A; **5**), 4,4′-dibromo-2,2′-thenil (green line, panel B; **6**), and 5,5′-dibromo-2,2′-thenil (cyan line, panel B; **7**).

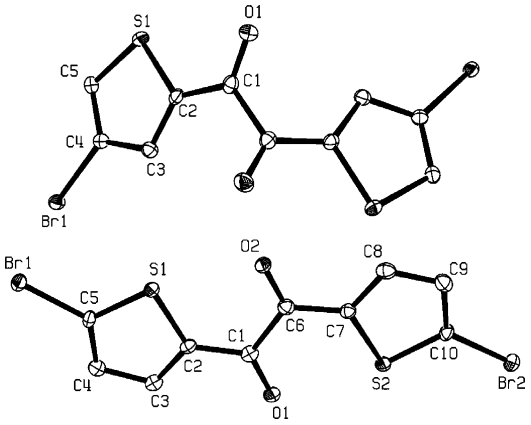

Figure 5. ORTEP depictions of 4,4′-dibromo-2,2′-thenil (top; **6**) and 5,5′-dibromo-2,2′-thenil (bottom; **7**).

P values for the particular esters.[40] However, no correlation was observed with this parameter and the K_i values for the dione inhibitors with r^2 values ranging from 0.19 to 0.28 for hiCE, hCE1, and rCE (data not shown). In contrast, good correlations were observed when comparing the empirical resonance energies, the aromatic energies based upon heat of union of nonaromatic precursors, or energy values derived from molecular orbital calculations, with the K_i values (Figure 1). As can be seen, r^2 correlates ranged from 0.84 to 0.97. This suggests that the stabilization of the aromatic rings enhances the potency of the inhibitors. Since the active site of CEs is lined with aromatic amino acids such as tyrosine and phenylalanine,[10] potentially π orbital stacking might occur between these residues and the aromatic rings in the inhibitors. This would lead to enhanced stabilization of enzyme/inhibitor complexes and should result in reduced K_i values for compounds that were 'more' aromatic. This is consistent with the results we observed.

Upon the basis of the correlation of aromaticity with potency of inhibition of CEs, we predicted that compounds that were more aromatic than benzene should be very good inhibitors of these enzymes. Using the equations derived from the data plotted in Figure 1, we predicted the K_i values for 2,2′-naphthil (**11**), the naphthalene derivative of benzil, with the different enzymes. This was achieved using the empirical resonance energy [31] (61 kcal/mol), the aromatic energy calculated from the heat of union of non aromatic precursors[32] (47.7 kcal/mol), or the resonance energy as calculated using MOPAC (41.6kcal/mol). While very low K_i values were predicted for hiCE and hCE1, the observed experimental values were much higher at 85 and 255 nM, respectively. In contrast, the predicted K_i values for rCE with 2,2′-naphthil were very close to the observed value. We believe that the discrepancy in the predictions for the human CEs with this compound are due to structural constraints afforded by the entrances to the active sites of these enzymes.[10] We have previously demonstrated that the active site entrance in rCE is considerably larger than in hiCE or hCE1.[10] It is likely therefore that 2,2′-naphthil (**11**) cannot readily gain access to the catalytic amino acids of the human enzymes that are buried at the bottom of a long gorge. However with rCE, access is not impeded, and hence the predicted K_i value closely matches that observed from the experimental studies.

It would be expected that compounds that adopt a fixed position suitable for interaction and inhibition of CEs would be more potent inhibitors than compounds that were highly flexible and mobile. We therefore assessed the mobility of the inhibitors by examining the rotation around the dione moiety using molecular dynamics. Analysis of these results indicated that diones that were better inhibitors demonstrated reduced rotation around this bond. This was exemplified for example, by comparison of 2,2′-naphthil (**11**) with 2,2′-furil (**9**). With the former compound, the rate of rotation around the dione dihedral was minimized after 1.5 ps, whereas with the latter inhibitor, the molecule was still rotating after 15 ps (Figure 2). In general, there was a correlation between the time taken for the rotation to become minimized and the K_i value, such that compounds that were better inhibitors demonstrated reduced mobility around the dione bond. While this may represent differences in the minimization parameters obtained from using the PM3 and MM3 Hamiltonian's, it is unclear why these molecular dynamics simulations allow identification of compounds with enhanced ability to inhibit CEs.

It was also noted that, in general, compounds that were better CE inhibitors adopted a final dione dihedral

angle of ~230° following the molecular dynamics simulations (Figures 2, 3, and 4). Since we have previously postulated that reactivity with the active site serine residue within CEs is important for enzyme inhibition,[21] it is likely that the conformation of the inhibitor when at this particular angle allows nucleophilic attack of the dione.

Similar results were observed with 2,2′-thenil (**4**) and 3,3′-thenil (**5**), with the former compound demonstrating lower K_i values, reduced mobility around the dione moiety, and a final dihedral angle close to 230° (Figure 4A). However, the mobility seen with bromine-substituted thenils (Table 2 and Figure 4B) did not correlate with enzyme inhibition. In these cases, increased flexing was seen in the molecular dynamics simulations that persisted for the entire 15 ps run (Figure 4B). Analysis of the contribution of halides to the aromaticity of the thiophene ring has been discussed by Sargent et al.[41] These authors reported that substitution at the 5-position of the ring might influence the distribution of the π electrons within the thiophene moiety. These theoretical studies suggest that the bromine atoms may disrupt the aromaticity of the rings due to π electron donation.[41] Our studies indicate that the halogen also influences the rotation around and the dihedral angle of the dione bond within the thenils, and hence both factors may contribute to the biological activity of these compounds. However, substitution of hydrogen atoms in the thiophene rings with bromine increased the potency of the molecules toward CE inhibition (Table 2). The most likely explanation for this is that the halogen atoms significantly increase the hydrophobicity of the molecules (log *P* values for the bromo analogues are 4.06, as compared to 2.77 for 2,2′-thenil, as calculated using ChemSilico Predict software (ChemSilico LLC, Tewkesbury, MA)). Previous studies with benzil analogues have indicated that substitution of either chlorine or bromine atoms within the aromatic rings, significantly reduces the K_i values for CE inhibition, likely due to enhanced affinity of the compound for the highly hydrophobic enzyme active site.[10,21,25] The results presented here with the 2,2′-thenil analogues are consistent with these previous observations.

Overall, our data suggests that the inhibition of CEs by aromatic diones is dependent upon the aromaticity of the rings and the flexibility of the molecules around the dione moiety. We are currently using these data to predict the ability of novel compounds to inhibit these enzymes, with the ultimate goal of designing and synthesizing potent, water soluble CE inhibitors.

Acknowledgment. This work was supported in part by an NIH Cancer Center Core Grant P30 CA-21765 (J.L.H., K.J.P.Y., M.W., C.C.E., M.K.D., P.M.P.), the American Lebanese Syrian Associated Charities (J.L.H., K.J.P.Y., M.W., C.C.E., M.K.D., P.M.P.), the Donors of the American Chemical Society Petroleum Research Fund (G.C.), Central Connecticut State University Faculty-Research Grants (V.S., G.C.) Central Connecticut State University Research Grants (V.S., G.C.), and NSF Grant 0111511 (M.Z., JU), and the diffractometer was funded by NSF grant 0087210, by Ohio Board of Regents Grant CAP-491, and by Youngstown State University.

Supporting Information Available: Elemental composition analysis of compounds **5**, **6**, and **7** and the full details of the crystal structure determinations for **6** and **7**. This material is available free of charge via the Internet at http://pubs.acs.org.

References

(1) Cashman, J.; Perroti, B.; Berkman, C.; Lin, J. Pharmacokinetics and molecular detoxification. *Environ. Health Perspect.* **1996**, *104*, 23−40.
(2) Brzezinski, M. R.; Abraham, T. L.; Stone, C. L.; Dean, R. A.; Bosron, W. F. Purification and characterization of a human liver cocaine carboxylesterase that catalyzes the production of benzoylecgonine and the formation of cocaethylene from alcohol and cocaine. *Biochem. Pharmacol.* **1994**, *48*, 1747−1755.
(3) Danks, M. K.; Morton, C. L.; Krull, E. J.; Cheshire, P. J.; Richmond, L. B.; Naeve, C. W.; Pawlik, C. A.; Houghton, P. J.; Potter, P. M. Comparison of activation of CPT-11 by rabbit and human carboxylesterases for use in enzyme/prodrug therapy. *Clin. Cancer Res.* **1999**, *5*, 917−924.
(4) Danks, M. K.; Potter, P. M. Enzyme-prodrug systems: carboxylesterase/CPT-11. *Methods Mol. Med.* **2004**, *90*, 247−262.
(5) Khanna, R.; Morton, C. L.; Danks, M. K.; Potter, P. M. Proficient metabolism of CPT-11 by a human intestinal carboxylesterase. *Cancer Res.* **2000**, *60*, 4725−4728.
(6) Pindel, E. V.; Kedishvili, N. Y.; Abraham, T. L.; Brzezinski, M. R.; Zhang, J.; Dean, R. A.; Bosron, W. F. Purification and cloning of a broad substrate specificity human liver carboxylesterase that catalyzes the hydrolysis of cocaine and heroin. *J. Biol. Chem.* **1997**, *272*, 14769−14775.
(7) Potter, P. M.; Wolverton, J. S.; Morton, C. L.; Wierdl, M.; Danks, M. K. Cellular localization domains of a rabbit and a human carboxylesterase: Influence on irinotecan (CPT-11) metabolism by the rabbit enzyme. *Cancer Res.* **1998**, *58*, 3627−3632.
(8) Satoh, T.; Hosokawa, M. The mammalian carboxylesterases: from molecules to function. *Annu. Rev. Pharmacol. Toxicol.* **1998**, *38*, 257−288.
(9) Satoh, T.; Hosokawa, M.; Atsumi, R.; Suzuki, W.; Hakusui, H.; Nagai, E. Metabolic activation of CPT-11, 7-ethyl-10-[4-(1-piperidino)-1-piperidino]carbonyloxycamptothecin, a novel antitumor agent, by carboxylesterase. *Biol. Pharm. Bull.* **1994**, *17*, 662−664.
(10) Wadkins, R. M.; Morton, C. L.; Weeks, J. K.; Oliver, L.; Wierdl, M.; Danks, M. K.; Potter, P. M. Structural constraints affect the metabolism of 7-ethyl-10-[4-(1-piperidino)-1-piperidino]carbonyloxycamptothecin (CPT-11) by carboxylesterases. *Mol. Pharmacol.* **2001**, *60*, 355−362.
(11) Guemei, A. A.; Cottrell, J.; Band, R.; Hehman, H.; Prudhomme, M.; Pavlov, M. V.; Grem, J. L.; Ismail, A. S.; Bowen, D.; Taylor, R. E.; Takimoto, C. H. Human plasma carboxylesterase and butyrylcholinesterase enzyme activity: correlations with SN-38 pharmacokinetics during a prolonged infusion of irinotecan. *Cancer Chemother. Pharmacol.* **2001**, *47*, 283−290.
(12) Morton, C. L.; Wierdl, M.; Oliver, L.; Ma, M.; Danks, M. K.; Stewart, C. F.; Eiseman, J. L.; Potter, P. M. Activation of CPT-11 in mice: Identification and analysis of a highly effective plasma esterase. *Cancer Res.* **2000**, *60*, 4206−4210.
(13) Morton, C. L.; Taylor, K. R.; Iacono, L.; Cheshire, P.; Houghton, P. J.; Danks, M. K.; Stewart, C. F.; Potter, P. M. Metabolism of CPT-11 in esterase deficient mice. *Proc. Am. Assoc. Cancer Res.* **2002**, *43*, 248.
(14) Potter, P. M.; Pawlik, C. A.; Morton, C. L.; Naeve, C. W.; Danks, M. K. Isolation and partial characterization of a cDNA encoding a rabbit liver carboxylesterase that activates the prodrug Irinotecan (CPT-11). *Cancer Res.* **1998**, *52*, 2646−2651.
(15) Bleiberg, H.; Cvitkovic, E. Characterisation and clinical management of CPT-11 (irinotecan)-induced adverse events: the European perspective. *Eur. J. Cancer* **1996**, *32A Suppl 3*, S18−23.
(16) Rivory, L. P. Irinotecan (CPT-11): a brief overview. *Clin. Exp. Pharmacol. Physiol.* **1996**, *23*, 1000−1004.
(17) Saliba, F.; Hagipantelli, R.; Misset, J. L.; Bastian, G.; Vassal, G.; Bonnay, M.; Herait, P.; Cote, C.; Mahjoubi, M.; Mignard, D.; Cvitkovic, E. Pathophysiology and therapy of irinotecan-induced delayed-onset diarrhea in patients with advanced colorectal cancer: a prospective assessment. *J. Clin. Oncol.* **1998**, *16*, 2745−2751.
(18) Beroza, P.; Villar, H. O.; Wick, M. M.; Martin, G. R. Chemoproteomics as a basis for post-genomic drug discovery. *Drug Discovery Today* **2002**, *7*, 807−814.
(19) Dixon, S. L.; Villar, H. O. Bioactive diversity and screening library selection via affinity fingerprinting. *J. Chem. Inf. Comput. Sci.* **1998**, *38*, 1192−1203.
(20) Dixon, S. L.; Villar, H. O. Investigation of classification methods for the prediction of activity in diverse chemical libraries.*J. Comput.-Aided Mol. Des.* **1999**, *13*, 533−545.

(21) Wadkins, R. M.; Hyatt, J. L.; Wei, X.; Yoon, K. J.; Wierdl, M.; Edwards, C. C.; Morton, C. L.; Obenauer, J. C.; Damodaran, K.; Beroza, P.; Danks, M. K.; Potter, P. M. Identification and characterization of novel benzil (diphenylethane-1,2-dione) analogues as inhibitors of mammalian carboxylesterases. *J. Med. Chem.* **2005**, *48*, 2905−2915.
(22) Mohrig, J. R.; Hammond, C. N.; Schatz, P. F.; Morrill, T. C., Thiamine-catalyzed benzoin condensation. In *Modern projects and experiments in organic chemistry: Miniscale and Williamson microscale*; W. H. Freeman & Co.: New York, 2003; pp 367−368.
(23) Weiss, M.; Appel, M. The catalytic oxidation of benzoin to benzil. *J. Am. Chem. Soc.* **1948**, *70*, 3666−3667.
(24) Morton, C. L.; Potter, P. M. Comparison of *Escherichia coli, Saccharomyces cerevisiae*, *Pichia pastoris*, *Spodoptera frugiperda* and COS7 cells for recombinant gene expression: Application to a rabbit liver carboxylesterase. *Mol. Biotechnol.* **2000**, *16*, 193−202.
(25) Wadkins, R. M.; Hyatt, J. L.; Yoon, K. J.; Morton, C. L.; Lee, R. E.; Damodaran, K.; Beroza, P.; Danks, M. K.; Potter, P. M. Identification of novel selective human intestinal carboxylesterase inhibitors for the amelioration of irinotecan-induced diarrhea: Synthesis, quantitative structure−activity relationship analysis, and biological activity. *Mol. Pharmacol.* **2004**, *65*, 1336−1343.
(26) Webb, J. L. *Enzyme and Metabolic Inhibitors. Volume 1. General Principles of Inhibition*; Academic Press Inc.: New York, 1963; p 57.
(27) Ellman, G. L.; Courtney, K. D.; Anders, V.; Featherstone, R. M. A new and rapid colorimetric determination of acetylcholinesterase activity. *Biochem. Pharmacol.* **1961**, *7*, 88−95.
(28) Doctor, B. P.; Toker, L.; Roth, E.; Silman, I. Microtiter assay for acetylcholinesterase. *Anal. Biochem.* **1987**, *166*, 399−403.
(29) Morton, C. L.; Wadkins, R. M.; Danks, M. K.; Potter, P. M. CPT-11 is a potent inhibitor of acetylcholinesterase but is rapidly catalyzed to SN-38 by butyrylcholinesterase. *Cancer Res.* **1999**, *59*, 1458−1463.
(30) Wadkins, R. M.; Potter, P. M.; Vladu, B.; Marty, J.; Mangold, G.; Weitman, S.; Manikumar, G.; Wani, M. C.; Wall, M. E.; VonHoff, D. D. Water soluble 20(S)-glycinate esters of 10,11-methylenedioxycamptothecins are highly active against human breast cancer xenografts. *Cancer Res.* **1999**, *59*, 3424−3428.
(31) Gordon, A. J.; Ford, R. A. *The Chemist's Companion: A handbook of practical data, techniques*; John Wiley and Sons: New York, 1972; and references therein.
(32) Dewar, M. J. S.; Holder, A. J. Atomic energies of some heteroaromatic compounds. *Heterocycles* **1989**, *28*, 1135−1156.
(33) Dewar, M. J. S.; DeLano, W. L. Ground states of conjugated molecules. XI. Improved treatment of hydrocarbons. *J. Am. Chem. Soc.* **1969**, *61*, 789−795.
(34) Stewart, J. J. MOPAC: a semiempirical molecular orbital program. *J. Comput.-Aided Mol. Des.* **1990**, *4*, 1−105.
(35) Stewart, J. J. P. Optimization of parameters for semiempirical methods. *J. Computat. Chem.* **1989**, *10*, 209−220.
(36) Sheldrick, G. M. SADABS. University of Gottingen, Gottingen, 1996.
(37) Sheldrick, G. M. *SHELXTL-Plus*; Madison, WI, 1990; p∧pp.
(38) Flack, H. D. On enantiomorph-polarity estimation. *Acta Crystallogr.* **1983**, *A39*, 876−881.
(39) Ferrugia, L. J. ORTEP-3 for Windows − a version of ORTEP−III with a Graphical User Interface (GUI). *J. Appl. Crystallogr.* **1997**, *30*, 565.
(40) Huang, T. L.; Szekacs, A.; Uematsu, T.; Kuwano, E.; Parkinson, A.; Hammock, B. D. Hydrolysis of carbonates, thiocarbonates, carbamates, and carboxylic esters of alpha-naphthol, beta-naphthol, and *p*-nitrophenol by human, rat, and mouse liver carboxylesterases. *Pharm. Res.* **1993**, *10*, 639−648.
(41) Sargent, A. L.; Titus, E. P.; Riordan, C. G.; Rheingold, A. L.; Ge, P. Poly(2-thienyl)borates: An investigation into the coordination of thiophene and its derivatives. *Inorg. Chem.* **1996**, *35*, 7095−7101.

JM0504196